



# Torsional wave dispersion and dissipation in solar tornados

A. Abdolhosseinzadeh<sup>1</sup>, Z. Fazel<sup>1</sup>, and S. Vasheghani Farahani<sup>2,\*</sup>

<sup>1</sup> Faculty of Physics, University of Tabriz, Tabriz, Iran

<sup>2</sup> Department of Physics, Tafresh University, Tafresh 39518 79611, Iran

Received 19 February 2026 / Accepted 12 April 2026

## ABSTRACT

**Aims.** We investigated the nature of solar atmosphere tornados hosting torsional Alfvén waves and fast magnetoacoustic torsional waves in the context of energy transport and transfer.

**Methods.** Solar tornados created by equilibrium magnetic twist and plasma rotation were modeled and studied analytically by implementing the resistive magnetohydrodynamic theory in cylindrical geometry. The dispersion relations were obtained by the second-order thin flux-tube approximation in the linear regime to enable us to consider damping effects connected with magnetic diffusivity and plasma viscosity.

**Results.** The obtained implicit dispersion relation provides a broad picture of the significance of the equilibrium and atmosphere conditions in addition to dissipative effects. The damping depends on the magnetic twist and plasma rotation in addition to the plasma- $\beta$  effects. The efficiency of damping due to magnetic diffusivity is enhanced by stronger equilibrium-twisted magnetic fields. The torsional fast magnetoacoustic wave is more affected by dispersion in the limit of zero plasma  $\beta$  in the presence of diffusive and viscous effects. The dispersion due to magnetic diffusivity is enhanced by the plasma  $\beta$ . The plasma viscosity enhances the efficiency of the plasma  $\beta$  regarding dispersion effects. The damping of torsional fast magnetoacoustic waves in solar tornados due to magnetic diffusivity is proportional to the equilibrium magnetic twist for photospheric and coronal conditions. The efficiency of damping is higher in photospheric conditions. The viscosity has a stronger damping effect in lower plasma- $\beta$  conditions. In photospheric conditions, the equilibrium magnetic twist has a stronger damping effect than in coronal conditions, when magnetic diffusivity and plasma viscosity are both present.

**Conclusions.** The model provides a theoretical basis for development of magnetohydrodynamic seismology of solar tornados. The combined dissipative effects we illustrate clearly show that the damping due to magnetic diffusivity is significantly enhanced in the presence of plasma viscosity. As damping is a feature of resistance, various modes dissipate subject to atmosphere conditions. This provides a sustainable heating mechanism in the solar atmosphere.

**Key words.** Sun: chromosphere – Sun: corona – Sun: magnetic fields – Sun: oscillations

## 1. Introduction

The solar corona possesses ordered and turbulent features that are constituted by magnetic fields that either rise from lower atmosphere levels or are locally induced in the corona. The framework of the solar atmosphere is based on magnetic fields that characterize local plasma structures. We modeled local plasma structures in the context of coronal heating by magnetohydrodynamic (MHD) waves (Alfvén & Lindblad 1947). We implemented the MHD theory (Goossens 2003) to model torsional fast wave propagation in solar atmosphere tornados in nonideal conditions. An important feature of the model we studied is its ability to highlight the interplay of dissipative damping connected with viscous plasmas (Nakariakov et al. 1999) and diffusive damping connected with magnetism (Wilmot-Smith et al. 2005; Matsuoka et al. 2024) in various situations and conditions of the solar atmosphere. The theoretical model we developed provides insight into oscillations linked to the initial conditions and local atmosphere situations connected to various layers of the solar atmosphere in the context of coronal heating. Coronal heating by MHD waves is achieved by thermal losses in addition to energy transfer mechanisms in

the solar atmosphere (Van Doorsselaere et al. 2020). Nonetheless, the seismological aspect (De Moortel & Nakariakov 2012) of energy losses and damping mechanisms connected with MHD waves in solar plasma structures is vital. The damping or stability of solar plasma structures depend on the heating mechanisms they experience. Important damping processes experienced by MHD waves in the solar atmosphere are resonant absorption (Ionson 1978; Goossens et al. 1992) and phase mixing (Heyvaerts & Priest 1983; Cargill et al. 2016) of MHD waves (Smith et al. 2007; Van Doorsselaere et al. 2020; Morton et al. 2023). The energy that is dissipated to the solar corona caused by enhanced phase mixing of torsional Alfvén waves becomes more significant in the presence of an anomalous viscosity (Boocock & Tsiklauri 2022b). Interestingly, fast magnetoacoustic waves that are generated by nonlinear Alfvén waves in the context of phase mixing are saturated depending on the strength of inhomogeneity (Tsiklauri et al. 2001). However, the mode conversion of nonlinear torsional Alfvén waves enables a mechanism for viscous damping that contributes to coronal heating (Boocock & Tsiklauri 2022a).

The heating mechanisms due to various damping models provide a prominent seismological tool for determining a specific set of coronal plasma parameters (Kolotkov et al. 2021) in addition to enabling us to trace the signature of solar convective motion to the corona (Morton & Soler 2025). The

\* Corresponding authors:  
S.Vasheghani.farahani@Tafreshu.ac.ir;  
Sofarahani@yahoo.com

magnetic field mediates the rotation of the plasma from the convection zone to the solar atmosphere (Kato & Wedemeyer 2017). This scenario is thought to create vortex or rotational motions in the solar atmosphere that are called tornados (Wedemeyer & Steiner 2014). This shows that rotational motions and the twisted magnetic fields are tightly correlated (Battaglia et al. 2021). This means that the combination of vortex flows and magnetic fields results in the twisted magnetic field lines that may form swirls that penetrate to higher altitudes in the solar atmosphere. Their lifetimes are between 90 and 2000 s (Dakanalis et al. 2022). Vesa et al. (2025) observed chromosphere swirls (Dakanalis et al. 2021) with the Dunn solar telescope with diameters of about 3.6 Mm, lifetimes of about 480 s, and oscillation periods of about 180 s. The authors suggested that the swirls contribute to coronal heating and that these vortex motions might be caused by torsional Alfvén waves. Torsional waves are connected with vortex flows that increase the dynamical pressure at the boundary of the magnetic cylinder, which acts as a wave guide that directs the wave energy to higher altitudes of the solar atmosphere (Skirvin et al. 2025). This statement is based on the effects connected to nonlinear forces, that is, ponderomotive, centrifugal, and magnetic tension (Vasheghani Farahani et al. 2011; Ghoraba & Farahani 2018; Belov et al. 2022).

For example, dissipation can be caused by ion–neutral collisions or friction (e.g. Kumar & Roberts 2003; Zaqarashvili et al. 2011; Russell & Fletcher 2013) in the chromosphere, which is inversely proportional to the expansion rate of the magnetic flux tube (Soler et al. 2017). Skirvin et al. (2025) suggested that vortex motions increase the plasma density at the tube boundaries and trap the wave energy more efficiently within the magnetic structure. This increases the magnetic energy transport to the outer layers of the solar atmosphere. Thus, the wave lifetimes become longer and the energy transfers last longer. Dissipation due to a specific mechanism depends on the atmosphere conditions hosting the wave propagation. For instance, the total resistive heating flux depends on the oscillation frequency (Leake et al. 2005; Goodman 2011). It is also known that the damping time for torsional waves due to viscous dissipation depends on the plasma  $\beta$  (Ghoraba & Farahani 2018), which is a measure of solar atmosphere pressure conditions ( $\beta = p/B^2/2\mu$ ) (Goossens 2003) and is also an indicator of the altitude from the solar surface (Aschwanden 2005). This motivated efforts to take effects into account that are connected with magnetic diffusivity, in addition to equilibrium effects such as magnetic twist and plasma rotation, which affect the oscillation frequency (Zhugzhda 1996; Vasheghani Farahani et al. 2010; Mozafari Ghoraba et al. 2018) and speed (Vasheghani Farahani et al. 2017).

To be more specific, the internal and external Alfvén wave speeds together with the internal and external density ratios might be estimated (Pascoe et al. 2016) if the loop length and the oscillation periods of the standing kink modes of the loop are measured by implementing an appropriate damping profile based on the observed oscillations of a solar loop. Zhong et al. (2023) compared various damping models applicable to various coronal loop conditions in order to estimate their transverse density profiles. The damping patterns act as a measure for validating seismological techniques based on the oscillation periods or the ratio of different parallel harmonics (Nakariakov et al. 2024). Interestingly, the magnetic field topology of active regions is expressed by the damping models (Selwa & Ofman 2010), where all are validated by the corresponding oscillations reported by observations (Aschwanden et al. 2002). It is worth noting that

Chae et al. (2008) focused on the interplay of the resolved plasma motions and magnetic diffusion to express the variations in the solar atmosphere magnetic fields. The seismological aspects of their work was to obtain plasma motion parameters together with the magnetic diffusivity by changes in the magnetic pattern.

In our study, the MHD wave we implemented as a seismological tool for studying solar tornados (Tziotziou et al. 2018) is the torsional polarized fast magnetoacoustic wave. We had two reasons for this choice based on the nature of the torsional fast magnetoacoustic wave. First, it possesses torsional polarization conveyed from the torsional Alfvén wave, where a solar cylindrical structure, for instance, enables alternate rotational motions together with an alternate twisting of the magnetic field (Nakariakov & Kolotkov 2020). Second, it possesses a collective behavior because the Alfvén wave speed is modified by the equilibrium magnetic twist and rotation of the solar magnetic cylindrical structure that hosts the MHD wave propagation (Zhugzhda & Nakariakov 1999; Vasheghani Farahani et al. 2010). Nonetheless, by detecting antiphase incompressible torsional oscillations propagating in pores located in the solar photosphere, Stangalini et al. (2021) emphasized the contribution of a torsional wave to energy transport in the solar atmosphere and solar wind acceleration. Tornados have also been observed to trigger coronal mass ejections (Mghebrishvili et al. 2018), which in turn created interest in studying the wave propagation in tornados.

In a numerical study, Soler et al. (2019) injected a wave with an energy flux of  $10^7 \text{ erg cm}^{-2} \text{ s}^{-1}$  from the solar photosphere with a background magnetic field of 1000 Gauss. They observed that through ohmic magnetic diffusion and ion–neutral collisions, only  $10^5 \text{ erg cm}^{-2} \text{ s}^{-1}$  of the energy flux reached the corona. The authors suggested that the variations in the maximum transmittance wave frequency is proportional to the background magnetic field. When the background magnetic field is 10 Gauss, about 50% of the Poynting flux connected to the solar magnetic tornados therefore reaches the corona and contributes to coronal heating. This contribution is directly proportional to the magnetic field strength (Kuniyoshi et al. 2023). It is illustrative to note that the chromosphere acts as a barrier for outward-propagating Alfvén waves, especially for those with periods shorter than a few seconds (De Pontieu et al. 2001).

In order to provide a theoretical basis for the development of MHD seismology by viscous damping, Nakariakov et al. (2000) provided expressions for the propagation of nonlinear magnetoacoustic slow waves in coronal loops and illustrated that the wave amplitudes become more damped by a stronger plasma viscosity. This agreed with the dissipation experienced by slow magnetoacoustic waves in the nonlinear regime due to wave steepening, which leads to enhanced dissipation in coronal plumes (Ofman et al. 1999, 2000). It was shown that the waves transferred their energy to the atmosphere before they reached one solar radius. This contributes to coronal heating. The model and conclusions proved so illustrative that when observations of solar rotating structures called swirls and tornados were reported by Komm et al. (2014), Wedemeyer & Steiner (2014), Kato & Wedemeyer (2017), motivation was provided to study torsional waves in solar tornados (Vasheghani Farahani et al. 2017) followed by studying the viscous damping of torsional waves in solar tornados (Mozafari Ghoraba et al. 2018), plumes (Hejazi et al. 2024), and loops (Hejazi et al. 2025). To do this, an initially rotating and twisted magnetic cylinder is immersed in a static magnetic medium that resembles a solar tornado (Fig. 1). The aim is to investigate the dominant damping mechanism

that a fast magnetoacoustic torsional wave experiences in various regions of the solar atmosphere (Khodachenko et al. 2004). For the aims of our study, a follow-up of the model presented by Mozafari Ghoraba et al. (2018) was carried out to provide expressions for the speed reduction and damping aspects of fast magnetoacoustic torsional waves in the presence of magnetic diffusivity before we compared the results with corresponding effects connected with the plasma viscosity. Mozafari Ghoraba et al. (2018) implemented the second-order thin flux tube approximation with transverse structuring in the presence of viscosity and gravity. They obtained an analytic dispersion relation to readily understand the effects of equilibrium conditions accompanied by plasma viscosity and gravity on the frequency and damping of fast magnetoacoustic waves.

We describe the MHD theory in its application to a typical solar atmosphere tornado in Sect. 2. In Sect. 3 we present the equilibrium and atmosphere conditions in the framework of the resistive MHD equations by implementing the second-order thin flux tube approximation in order to provide the linearized set of equations. In Sect. 4 we present the implicit dispersion relation, which provides information regarding the equilibrium rotation and magnetic twist in addition to the atmosphere conditions and dissipative effects. We also present explicit dispersion relations to provide much simpler expressions of the interplay of the various physical conditions we considered. In Sect. 5 we discuss the dissipation and damping of torsional waves that propagate in solar tornados before we conclude in Sect. 6.

## 2. Theory and MHD set of equations

We implemented the MHD theory to provide implicit and explicit expressions regarding the propagation of fast magnetoacoustic torsionally polarized waves in solar tornados. To do this, we embedded a magnetized and rotating cylindrical plasma structure in a static magnetic medium to illustrate a solar tornado (Fig. 1) in the solar atmosphere (see also Vasheghani Farahani et al. 2017; Mozafari Ghoraba et al. 2018). We followed the model developed by Mozafari Ghoraba et al. (2018) by considering effects connected with magnetic diffusivity ( $\eta$ ) instead of solar gravity. Thus, the implemented MHD set of equations reads (Goossens 2003)

$$\rho \left( \frac{\partial \mathbf{v}}{\partial t} + (\mathbf{v} \cdot \nabla) \mathbf{v} \right) = -\nabla p + \rho \nu \left[ \nabla^2 \mathbf{v} + \frac{1}{3} \nabla (\nabla \cdot \mathbf{v}) \right] + \frac{1}{4\pi} (\nabla \times \mathbf{B}) \times \mathbf{B}, \quad (1)$$

$$\frac{\partial \rho}{\partial t} + \nabla \cdot (\rho \mathbf{v}) = 0, \quad (2)$$

$$\frac{\partial \mathbf{B}}{\partial t} = \nabla \times (\mathbf{v} \times \mathbf{B}) + \eta \nabla^2 \mathbf{B}, \quad (3)$$

together with the equation of state, which in the adiabatic conditions of our study results in  $p = C_S^2 \rho$  and the nonexistence of the magnetic monopole condition ( $\nabla \cdot \mathbf{B} = 0$ ) (see also Aschwanden 2005). We note that  $C_S$  represents the sound speed, and  $p$  and  $\rho$  represent the plasma pressure and density, respectively. The effects connected with kinematic viscosity ( $\nu$ ) are clearly reflected in the second term of the right-hand side of Eq. (1), while the effects connected with magnetic diffusivity ( $\eta$ ) are reflected in the second term of the right-hand side of Eq. (3).

In order to find illustrative relations that shed light on the character of various MHD waves propagating in a solar plasma structure, Eqs. (1)–(3) were linearized around the existing equilibrium. We choose the term “various MHD waves” because the

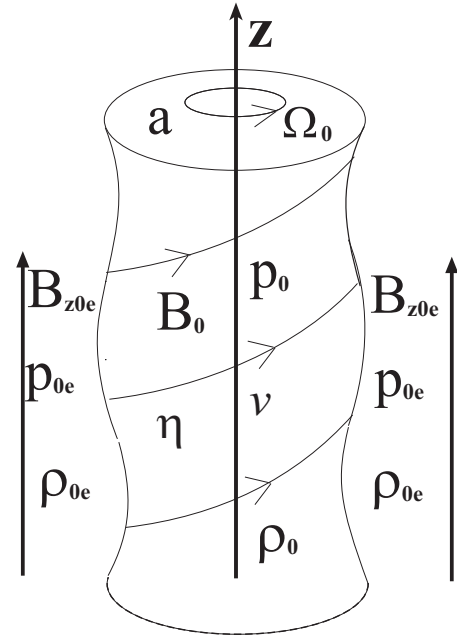


Fig. 1. Sketch of a solar tornado as considered here.

types of waves are subject to equilibrium and atmosphere conditions (Edwin & Roberts 1983; Nakariakov & Roberts 1995). To describe the nature of the MHD waves, Alfvén waves are driven by the magnetic tension force, while magnetoacoustic waves are driven by magnetic tension and pressure forces. Alfvén waves do not perturb the density in the linear regime, but magnetoacoustic waves do (Goossens 2003).

## 3. Linearized set of equations for torsional waves in tornados

Since a tornado possesses an equilibrium rotation and magnetic twist, the Alfvén speed would not be observed (Zhugzhda 1996; Zhugzhda & Nakariakov 1999) because the speed is modified to a fast magnetoacoustic speed (Vasheghani Farahani et al. 2010, 2017; Mozafari Ghoraba et al. 2018). We therefore need to focus more on effects connected with the equilibrium magnetic twist and rotation in various layers of the solar atmosphere with different dissipative conditions, namely viscosity and magnetic diffusivity. Therefore, the linearized set of equations was obtained by substituting the Taylor expansions of the variables up to their second-order terms (see, e.g., Zhugzhda 1996; Vasheghani Farahani et al. 2010; Mozafari Ghoraba et al. 2018),

$$\frac{\partial \Omega}{\partial t} + 2V_r \Omega_0 + \frac{J_0}{4\pi\rho_0} \frac{\partial B_z}{\partial z} - \frac{B_{z0}}{4\pi\rho_0} \frac{\partial J}{\partial z} - \nu \frac{\partial^2 \Omega}{\partial z^2} = 0, \quad (4)$$

$$\rho_0 \frac{\partial u}{\partial t} + \frac{\partial p}{\partial z} - \frac{2}{3} \rho_0 \nu \left( \frac{\partial V_r}{\partial z} + 2 \frac{\partial^2 u}{\partial z^2} \right) = 0, \quad (5)$$

$$\frac{\partial \rho}{\partial t} + \rho_0 \frac{\partial u}{\partial z} + 2\rho_0 V_r = 0, \quad (6)$$

$$\frac{\partial J}{\partial t} + 2V_r J_0 + J_0 \frac{\partial u}{\partial z} - B_{z0} \frac{\partial \Omega}{\partial z} - \eta \frac{\partial^2 J}{\partial z^2} = 0, \quad (7)$$

$$\frac{\partial B_z}{\partial t} + 2B_{z0} V_r - \eta \frac{\partial^2 B_z}{\partial z^2} = 0, \quad (8)$$

where  $J = B_\varphi/r$  and  $\Omega = V_\varphi/r$  represent the perturbations of the current density and vorticity, respectively. To state this more clearly,  $J$  and  $\Omega$  come from the Taylor expansion of  $B_\varphi$  and  $V_\varphi$  as zeroth-order terms, while  $V_r$  is the first-order derivative of the radial velocity with respect to the radial component. These terms do not depend on the radius (see [Zhugzhda 1996](#); [Vasheghani Farahani et al. 2010](#) for details). In the process of obtaining the linearized MHD equations, Eqs. (4)–(8), we focused on axisymmetric perturbations for which the partial derivative  $\partial/\partial\varphi$  of any variable results in zero. The effects connected with solar gravity are beyond the scope of this study. In addition to the nondependence on the radial component, only Eq. (5) out of Eqs. (4)–(6) is therefore different from its corresponding Euler equation (Eq. (8)) of [Mozafari Ghoraba et al. \(2018\)](#) because of the Taylor expansion. Because viscous effects are not the only resistive effects of interest in this study, magnetic diffusivity also feature in Eqs. (7) and (8), which are additional terms in comparison to their corresponding induction equations of [Mozafari Ghoraba et al. \(2018\)](#). We note that the zero index for the variables indicates their equilibrium values. In order to write the dispersion relation for fast magnetoacoustic torsional waves propagating in a solar tornado constituted by effects connected with vortices, magnetic twisted fields, resistive actors, and atmosphere conditions, we proceeded by installing two boundary conditions. The pressure balance at the tornado boundary and the continuity of the Lagrangian displacement at the tornado boundary result in

$$p + \frac{B_{z0}B_z}{4\pi} - \frac{A_0\rho_0}{2\pi} \frac{\partial V_r}{\partial t} + \frac{A_0\Omega_0^2\rho}{2\pi} + \frac{\rho_0\Omega_0^2 A}{2\pi} + \frac{A_0\rho_0\Omega_0\Omega}{\pi} - \frac{A_0J_0J}{4\pi^2} - \frac{A_0B_{z0}}{16\pi^2} \frac{\partial^2 B_z}{\partial z^2} - \frac{J_0^2 A}{8\pi^2} + \frac{A_0\rho_0\nu}{2\pi} \frac{\partial^2 V_r}{\partial z^2} = 0, \quad (9)$$

where  $A_0 = \pi a^2$  is the area of the tornado cross section at equilibrium as  $a$  represents its radius, while  $A$  represents the perturbations of the tornado cross section. Although the pressure balance at the tube boundary looks similar to Eq. (15) of [Mozafari Ghoraba et al. \(2018\)](#), the perturbations of the physical values differ because of the magnetic diffusivity observed in Eqs. (7) and (8).

#### 4. Dispersion relations

The backbone of every theoretical model regarding wave dynamics is the dispersion relation. The dispersion relation for wave propagation in tornados we considered was obtained by considering the perturbations proportional to  $\exp(i\omega t + ikz)$  before we combined Eqs. (4)–(8) with the relation governing the boundary conditions of the tornado expressed by Eq. (9). Thus, we obtained

$$\left[ \omega^6 - 2i\left(\frac{5}{3}\nu + \eta\right)k^2\omega^5 + \left(2C_A^2\alpha^2 - 4\Omega_0^2 - k^2\left(2C_A^2 + C_S^2 + \left(\eta^2 + \frac{20}{3}\eta\nu + \frac{11}{3}\nu^2\right)k^2\right)\right)\omega^4 + a\omega^3 + b\omega^2 + c\omega + \left(C_A^2C_S^2k^4\left(2\Omega_0^2 + 2\alpha^2C_A^2 - C_A^2k^2 - 2\alpha^2\eta\nu k^2 - 2\eta\nu k^4\right) + 2\Omega_0^2\eta\left(C_S^2\nu - C_A^2\nu - 2C_S^2\eta\right)k^6 \right. \right.$$

$$\left. - \eta^2\nu^2\left(C_S^2k^2 + 2\Omega_0^2\right)k^8\right] + 8i\alpha\Omega_0C_A^2C_S^2\eta k^5 \left[ - \left(\frac{4\pi\left(\omega^2 - k^2C_A^2\right)}{A_0}\right)\left(\left(C_A^2 + C_S^2\right)\left(\omega^2 - k^2C_T^2\right) - \frac{4}{3}iC_A^2\nu\omega k^2 - 2C_S^2\eta\nu k^4 - 2iC_S^2\left(\eta + \nu\right)k^2\omega\right) + \frac{4\pi\left(\eta + \nu\right)}{A_0}\left(\frac{1}{3}C_A^2\nu k^4\omega^2 + C_S^2\left(\eta + \nu\right)k^4\omega^2 + iC_A^2k^2\omega^3 - 2iC_S^2\eta\nu k^6\omega\right) + \frac{4\pi\nu}{A_0}\left(\left(2\eta + \nu\right)C_A^2\omega^2 - C_S^2\eta^2\nu k^4 - \frac{4}{3}iC_A^2\eta\nu k^2\omega\right)k^4 = 0, \quad (10)$$

where  $a$ ,  $b$ , and  $c$  are presented as

$$a = \left(\frac{2i}{3}\nu\left(2\nu^2 + 11\eta\nu + 5\eta^2\right)k^6 + 2i\left(C_S^2\left(\eta + \nu\right) + C_A^2\left(\frac{7}{3}\nu + \eta\right)\right)k^4 + 4C_A^2\alpha\Omega_0k + 2i\left(\Omega_0^2\left(\frac{7}{3}\nu + 5\eta\right) - C_A^2\alpha^2\left(\frac{5}{3}\nu + \eta\right)\right)k^2, \quad (11)$$

$$b = \left(2\left(\Omega_0^2C_S^2 + C_A^2C_S^2\alpha^2 - C_A^4\alpha^2\right)k^2 + C_A^2\left(2C_S^2 + C_A^2\right)k^4 + 2\Omega_0^2\left(3\eta^2 + 7\eta\nu - \frac{1}{3}\nu^2\right)k^4 - iC_A^2\alpha\Omega_0\left(\frac{20}{3}\nu + 4\eta\right)k^3 + \left(C_S^2\left(\nu^2 + 4\eta\nu + \eta^2\right) + \frac{2}{3}C_A^2\nu\left(4\nu + 7\eta\right)\right)k^6 + \frac{1}{3}\left(-2C_A^2\alpha^2\left(2\nu^2 + 5\eta\nu\right) + \nu^2\eta\left(8\nu + 11\eta\right)k^4\right)k^4 \right) \quad (12)$$

$$c = \left(-2iC_S^2\left(\eta + \nu\right)\left(C_A^2k^2 + \eta\nu k^4 + C_A^2\alpha^2\right)k^4 - 4\Omega_0\alpha C_A^2\left(2C_S^2 + \frac{5}{3}\eta\nu k^2\right)k^3 - \frac{4}{3}i\nu^2\eta\left(\nu\eta k^2 + 2C_A^2\right)k^8 - \frac{4}{3}iC_A^4\nu\left(k^2 - 2\alpha^2\right)k^4 + \frac{4}{3}i\left(C_A^2\alpha^2 - \Omega_0^2\right)\eta\nu^2k^6 + 2i\Omega_0^2\left(C_S^2\left(\nu - 3\eta\right) - C_A^2\left(\eta - \frac{\nu}{3}\right) - \frac{14}{3}\eta^2\nu k^2\right)k^4, \quad (13)$$

and  $C_A$  is the Alfvén wave speed, while the parameter  $\alpha$  that is equal to  $J_0/B_{z0}$  is a reference for the strength of the magnetic twist. The sixth-order dispersion relation represented by Eq. (10) possesses very interesting terms regarding various aspects of wave dynamics in solar atmosphere magnetic structures. It clearly provides information regarding atmosphere conditions in addition to the effects connected with the equilibrium magnetic twist and rotation by  $\alpha$  and  $\Omega_0$ , and dissipative effects via  $\nu$  and  $\eta$  on wave propagation and energy transfer. The energy transfer arises from the imaginary terms constituted by resistive and diffusive terms. In ideal conditions, Eq. (10) would lead to Eq. (12) of [Vasheghani Farahani et al. \(2010\)](#), who focused on modifying the speeds and the compressibility of the torsional wave caused by the magnetic twist and rotation. Eq. (10) is an implicit dispersion relation that is a functional relation between wave frequency ( $\omega$ ) and wave number ( $k$ ), expressed as  $f(\omega, k) = 0$ , where the frequency cannot be directly isolated. These equations often require numerical methods to solve for eigenvalues because the frequency-wave number dependence is embedded within transcendental or complex functions and is not

explicitly given as  $\omega = f(k)$ , which is an explicit dispersion relation. In addition, the effects of the variables in implicit relations appeared after we provided the curves and compared them in various conditions as their effects cannot be readily understood just by glancing at the relation. We therefore present the curves by numerically solving Eq. (10) by MATLAB in the figures below. We first defined the symbolic variables before we defined the dispersion relation (Eq. (10)) as a symbolic equation while providing values according to parameters connected with various atmosphere conditions, namely, plasma viscosity, magnetic diffusivity, plasma  $\beta$ , the equilibrium magnetic twist, and plasma rotation. We then converted the symbolic function into a numeric function to enable the contour command to plot the figures.

Although the Alfvén and sound speeds provide an impression of the atmosphere conditions due to their definition, it is illustrative to use the plasma  $\beta$ , which is their ratio ( $C_S^2/C_A^2$ ), to readily express their role in frequency, damping, and phase-speed dependences for various physical parameters. For an initially untwisted and nonrotating magnetic plasma structure experiencing magnetic diffusivity, we therefore obtained without loss of generality an approximate explicit relation for the dispersion of the fast torsional speed,

$$C_+ = C_A - \frac{\eta^2 k^2}{8C_A} + \frac{i\eta k}{2}, \quad (14)$$

where  $C_+$  represents the speed of the torsional Alfvén wave. The third term on the right-hand side of Eq. (14) expresses the damping due to magnetic diffusivity,

$$\gamma = \frac{\eta k^2}{2}. \quad (15)$$

The fast speed dispersion expressed by Eq. (14) clearly shows that the propagation of the torsional Alfvén wave is affected by the magnetic diffusivity. As expected, the plasma  $\beta$  does not appear in the dispersion relation since the Alfvén wave is independent of the sound speed.

In case of a twisted and rotating magnetic plasma structure that experiences magnetic diffusivity, the fast torsional speed is expressed by an explicit expression,

$$C_+ \simeq C_A \left( \frac{(1 + \mathcal{R} - \mathcal{K})(1 + \sqrt{\mathcal{K}\mathcal{R}})}{1 - \mathcal{K} + 2\mathcal{R}} \right) - \frac{0.15k^2\eta^2}{C_A(1 - \mathcal{K} + 2\mathcal{R})} + \eta k \left( \frac{0.3\sqrt{\mathcal{K}\mathcal{R}} - 0.3\mathcal{R} + 0.3\mathcal{K}}{1 - \mathcal{K} + 2\mathcal{R}} \right). \quad (16)$$

The damping of the torsional wave is expressed as

$$\gamma \simeq \frac{\eta k^2}{2} \left( \frac{1 + 5\mathcal{R} - 2\mathcal{K} - 0.6\sqrt{\mathcal{K}\mathcal{R}}}{1 - \mathcal{K} + 2\mathcal{R}} \right). \quad (17)$$

Equation (16) is an explicit relation that expresses the dispersion of the fast torsional wave speed based on the equilibrium magnetic twist and plasma rotation in addition to dissipative effects connected with the magnetic diffusivity in the zero-plasma- $\beta$  regime. This is in a sense that the first term on the left-hand side shows the effects of the equilibrium magnetic twist and rotation on the speed of the fast torsional magnetoacoustic wave. If we were to consider  $\mathcal{K} = A_0\alpha^2/2\pi$  and  $\mathcal{R} = A_0\Omega_0^2/2\pi C_A^2$  equal to zero in the long wavelength limit ( $k = 0$ ), it would simply result in the Alfvén speed  $C_A$ . The second and third terms illustrate the interplay of the equilibrium magnetic twist and plasma rotation on the modification of the fast speed and dispersion caused by magnetic diffusivity. Equation (17) represents the imaginary

term and indicates the damping caused by the magnetic diffusivity, which could vary due to the effects connected with equilibrium magnetic twist and plasma rotation.

In order to illustrate the joint effects connected with the equilibrium magnetic twist and magnetic diffusivity on speed and damping of the fast torsional wave, we obtained an explicit relation by switching off the equilibrium rotation ( $\mathcal{R} = 0$ ) in Eq. (16). The result was

$$C_+ \simeq C_A - \frac{0.15k^2\eta^2}{C_A(1 - \mathcal{K})} + \eta k \left( \frac{0.3\mathcal{K}}{1 - \mathcal{K}} \right), \quad (18)$$

which clearly shows that the speed of the torsional Alfvén wave in ideal conditions and in the long-wavelength limit is not affected by the equilibrium magnetic twist (see also [Vasheghani Farahani et al. 2010](#); [Ghoraba & Farahani 2018](#)). The damping of the torsional wave is expressed as

$$\gamma \simeq \frac{\eta k^2}{2} \left( \frac{1 - 2\mathcal{K}}{1 - \mathcal{K}} \right). \quad (19)$$

The damping is clearly dependent on the equilibrium magnetic twist. To present a better impression of the benefits and advantages of the dispersion relations and their contribution to seismology, we proceed and provide snapshots of the oscillations and damping based on various atmosphere parameters and equilibrium conditions.

## 5. Results and discussion

The dispersion relation expressed by Eq. (10) informs us about the effects connected with the equilibrium magnetic twist and plasma rotation on torsional wave propagation in dissipating solar tornados. The origin of solar vortices or tornados lies in either a rotating cylindrical plasma structure or a twisted magnetic cylindrical structure. [Silva et al. \(2021\)](#) expressed an appropriate classification based on their magnetic nature, called M-vortex, or based on the kinetic nature, called K-vortex. The M-vortices are then divided into two types, namely I and II, based on the ratio of the magnetic and kinetic energies. M-vortex types I or II represent a ratio that is higher or lower than unity. The plasma  $\beta$  is also a constituent of the dispersion relation (Eq. (10)) that represents the dominant pressure gradient in various layers of the solar atmosphere. The plasma- $\beta$  conditions reflect the presence of various types of vortices. This means that low plasma- $\beta$  regions host K-vortices, while higher plasma- $\beta$  regions host M-vortices [Silva et al. \(2021\)](#). The primary advantage of Eq. (10) therefore is that it enables snapshots of the interplay of various actors, especially the plasma  $\beta$ , which characterize the wave in its location. The red and yellow curves in Fig. 2 indicate that for coronal conditions in the zero-plasma- $\beta$  limit, the torsional Alfvén wave and the torsional fast magnetoacoustic wave are both slower in shorter wavelengths as a result of magnetic diffusivity. The speed for both waves is proportional to the wavelength in the presence of magnetic diffusivity in the zero-plasma- $\beta$  limit. Figure 2 also shows that the equilibrium magnetic twist ( $\mathcal{K}$ ) further reduces the phase speed for shorter wavelengths. The equilibrium magnetic twist modifies the Alfvén wave so that it becomes a fast magnetoacoustic wave ([Zhugzhda & Nakariakov 1999](#); [Vasheghani Farahani et al. 2010, 2017](#)).

In ideal conditions, it is known that equal values of the equilibrium magnetic twist ( $\mathcal{K}$ ) and plasma rotation ( $\mathcal{R}$ ) cancel out their effects and leave the phase speed of the torsional Alfvén wave unmodified ([Vasheghani Farahani et al.](#)

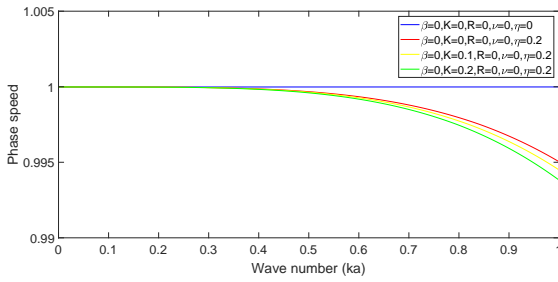


**Fig. 2.** Comparison of the phase speed of the torsional Alfvén wave and the torsional fast magnetoacoustic wave in the presence of magnetic diffusivity. The blue line represents the phase speed of the torsional Alfvén wave in ideal conditions. The red curve illustrates the effect of magnetic diffusivity on various wavelengths of the torsional Alfvén wave speed. The yellow and green curves represent the phase speed of the torsional wave when the equilibrium magnetic twist  $\mathcal{K}$  is equal to 0.1 and 0.2, respectively. The speeds are normalized by the torsional Alfvén wave speed.

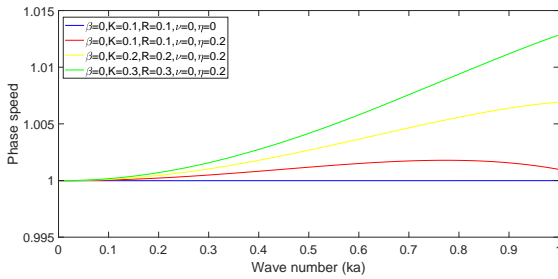


**Fig. 3.** Role of magnetic diffusivity in unbalancing the plasma rotation and magnetic twist, resulting in variations in the torsional wave phase speed. The blue line represents the phase speed of the torsional Alfvén wave, and the red, yellow, and green curves represent the phase speeds of fast magnetoacoustic torsional waves when the plasma rotation and magnetic twist are equal to 0.1, 0.2, and 0.3, respectively.

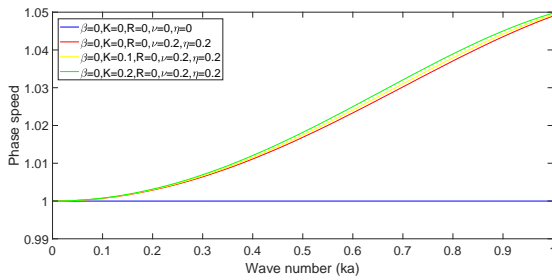


**Fig. 4.** Combined effect of magnetic diffusivity and plasma viscosity on the phase speed of fast magnetoacoustic torsional waves. The blue line represents the phase speed of the torsional Alfvén wave in ideal conditions, and the red, yellow, and green curves represent the phase speeds of fast magnetoacoustic torsional waves in resistive conditions when the magnetic twist is equal to 0, 0.1, and 0.2, respectively.

2017; Mozafari Ghoraba et al. 2018). Unlike when the solar tornado has only equilibrium twisted magnetic fields without rotation Fig. 2, however, the presence of equilibrium rotation creates a condition in which the phase speed increases for shorter wavelengths (Fig. 3). The reason lies in the nature of fluid rotation in the presence of magnetic fields when a negative diffusivity comes in to play (see also Bacri et al. 1995 regarding negative viscosity). Consequently, negative viscosity is apparent from

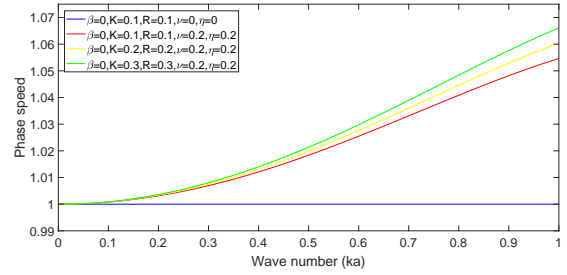


**Fig. 5.** Combined effect of magnetic diffusivity and plasma viscosity in unbalancing the plasma rotation and magnetic twist, resulting in variations in the torsional wave phase speed. The values for the magnetic twist and plasma rotation are the same as in Fig. 3.

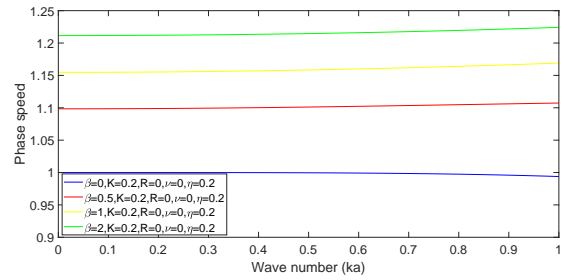


**Fig. 6.** Efficiency of the plasma  $\beta$  in the presence of equilibrium magnetic twist on the phase speed and dispersion of torsional fast magnetoacoustic waves. The blue, red, yellow, and green curves show plasma- $\beta$  values equal to 0, 0.5, 1, and 2, respectively.

comparison of the corresponding curves of Figs. 2 and 3 with Figs. 4 and 5, where in the zero-plasma- $\beta$  limit, equilibrium rotation (Fig. 5) causes the viscosity to further enhance the phase speed of torsional waves in shorter wavelengths. Moreover, the modification of the phase speed of fast magnetoacoustic torsional waves at shorter wavelengths is enhanced by the plasma  $\beta$ . In addition to this, Fig. 6 also illustrates the sense in which the equilibrium magnetic twist elevates the phase speed of the fast magnetoacoustic torsional wave in various layers of the solar atmosphere. In other words, the efficiency of the magnetic twist is proportional to the plasma  $\beta$ . The modification of the phase speed propagating in a solar tornado clearly highly depends on the solar atmosphere conditions and oscillation wavelength.

Furthermore, as the plasma  $\beta$  increases, the degree of imbalance caused by the equilibrium magnetic twist and plasma rotation is enhanced when the magnetic diffusivity is supplemented by plasma viscosity. A comparison between Figs. 7 and 8 proves adequate for this statement. The blue, red, yellow, and green curves represent the phase speed and dispersion of the fast magnetoacoustic waves for coronal, chromospheric, and photospheric conditions. However, the phase speed of fast magnetoacoustic waves in the long-wavelength limit stay unchanged.

The seismological point is that the phase speed of the torsional wave in a magnetically twisted tornado is reduced when it gains altitude. However, the seismological aspect might be fulfilled by understanding the damping situation. Fortunately, the scale of damping together with the actors affecting the damping are present in the dispersion relation (Eq. (10)).

The damping of the torsional Alfvén wave due to magnetic diffusivity is enhanced when the plasma  $\beta$  increases. In other words, the damping is directly proportional with the plasma  $\beta$ , where the elevation of the curves represented by red ( $\beta = 0.5$ ),

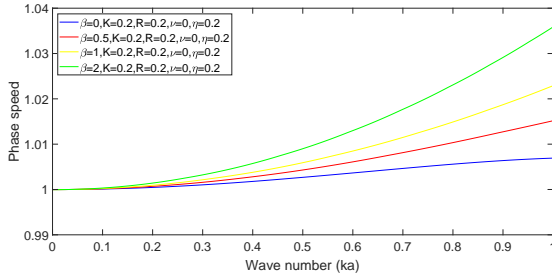


**Fig. 7.** Efficiency of magnetic diffusivity regarding the atmosphere effects connected with various plasma- $\beta$  conditions. The blue, red, yellow, and green curves represent the plasma- $\beta$  values equal to 0, 0.5, 1, and 2, respectively. The values for magnetic twist and plasma rotation are the same as in Fig. 3.

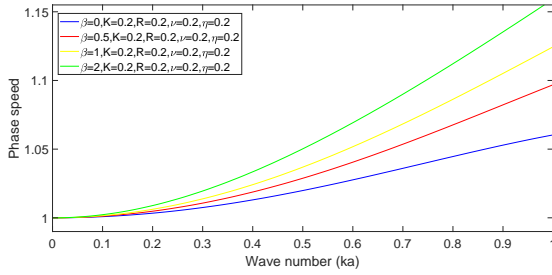


**Fig. 8.** Combined effect of magnetic diffusivity and plasma viscosity in unbalancing the plasma rotation and magnetic twist, resulting in torsional wave phase speed variations. The blue, red, yellow, and green curves represent plasma- $\beta$  values equal to 0, 0.5, 1, and 2, respectively. The values for magnetic twist and plasma rotation are the same as in Fig. 3.

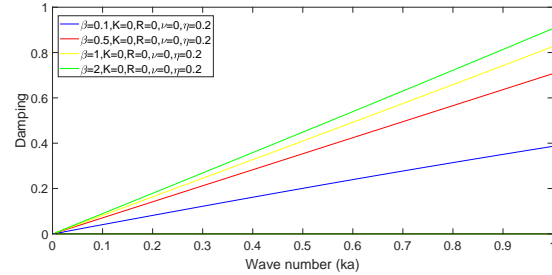


**Fig. 9.** Effect of plasma  $\beta$  on the efficiency of damping by magnetic diffusivity for an initially static tornado. The blue, red, yellow, and green curves represent the damping against wave number for torsional Alfvén waves at plasma- $\beta$  values of 0.1, 0.5, 1, and 2, respectively.

yellow ( $\beta = 1$ ), and green ( $\beta = 2$ ) compared to the blue curve ( $\beta = 0.1$ ) is shown in Fig. 9. This means that the damping of the torsional Alfvén wave due to magnetic diffusivity is more probable in photospheric conditions. In Fig. 10 we show two plasma- $\beta$  values. One value is 0.1, plotted as solid lines. It represents coronal conditions, and the other value is 1, plotted as dotted lines. It represents photosphere conditions. The equilibrium magnetic twist clearly enhances the damping due to magnetic diffusivity in photospheric and coronal conditions: the solid and dotted red curves lie above the corresponding blue curves with an almost similar elevation. When we consider the effects connected with plasma viscosity in addition to magnetic diffusivity, the damping is clearly stronger for photospheric than for coronal conditions. This is shown by the solid and dashed lines in Fig. 11.

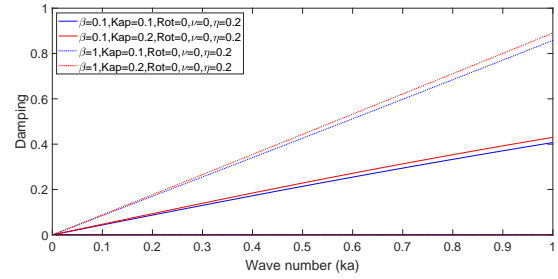


**Fig. 10.** Effect of magnetic twist on the efficiency of damping by magnetic diffusivity for an initially twisted tornado. The blue and red curves represent the damping against wave number regarding the fast magnetoacoustic torsional waves when the equilibrium magnetic twist is equal to 0.1 and 0.2, respectively. The solid and dotted curves show plasma- $\beta$  conditions equal to 0.1 and 1, respectively.

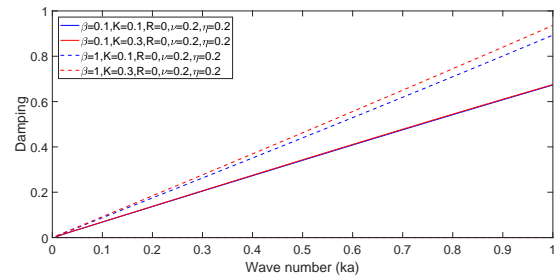


**Fig. 11.** Effect of magnetic twist on the efficiency of damping by the interplay of magnetic diffusivity and plasma viscosity for an initially twisted tornado. The blue and red curves represent the damping against wave number regarding the fast magnetoacoustic torsional waves when the equilibrium magnetic twist is equal to 0.1 and 0.3, respectively. The solid and dashed curves are for plasma- $\beta$  conditions equal to 0.1 and 1, respectively.

## 6. Conclusions

We studied torsional polarized wave damping in solar vortices or tornados in the context of chromospheric and coronal heating. The dominant damping actor depends on the atmosphere conditions through which the wave propagates [Khodachenko et al. \(2004\)](#). The total number of expected vortices at any time in the solar photosphere is estimated to be about  $1.48 \times 10^6$ . This indicates that 2.8% of the solar photosphere is constantly covered by vortices [Giagkiozis et al. \(2018\)](#), which proves adequate for their role in transferring energy to the solar corona. Further focus is required to model them theoretically. In the context of energy transfer by MHD waves, we modeled a solar tornado that hosts torsional polarized wave propagation. The tornado experienced magnetic diffusivity and plasma viscosity as moved to higher altitudes of the solar atmosphere. The resistive MHD set of equations was linearized before we took the boundary conditions of a magnetic twisted and rotating cylindrical structure into account in order to present the dispersion relation. The dispersion relation subject to conditions provides valuable information regarding the efficiency of various actors in the solar photosphere, chromosphere, and corona for the energy transfer by torsional waves. Our results are summarized below.

1. A well-developed dispersion relation (Eq. (10)) was derived that enabled us to focus on the oscillations and damping of torsional Alfvén waves and torsional fast magnetoacoustic waves. The dispersion relation is robust because it is constituted by terms that reflect the effects connected with

equilibrium magnetic twist and plasma rotation in addition to resistive terms, namely magnetic diffusivity and plasma viscosity in various layers of the solar atmosphere.

2. Explicit relations were obtained to express the speed dependence on the wavelength in the presence of magnetic diffusivity in various conditions of the solar atmosphere. These expressions enabled us to gauge the efficiency of damping in various equilibrium conditions for torsional wave propagation and damping in solar tornados.
3. For torsional Alfvén waves, the efficiency of damping due to magnetic diffusivity increases for more strongly twisted magnetic fields. Although the equilibrium magnetic twist does not affect the torsional Alfvén wave frequency in the zero plasma- $\beta$  limit (Vasheghani Farahani et al. 2010; Mozafari Ghoraba et al. 2018), the magnetic diffusivity enables the equilibrium magnetic twist to reduce the Alfvén wave speed, especially in shorter wavelengths (Fig. 2).
4. The balance between equilibrium magnetic twist and plasma rotation is violated by the magnetic diffusivity. This means that stronger magnetic twists and plasma rotations further enhance the torsional Alfvén wave speed in shorter wavelengths (Fig. 3). This corresponds to a negative magnetic diffusivity effect, which confirms the observations of Bacri et al. (1995) regarding negative viscosity effects. Moreover, the plasma viscosity further increases the phase speeds for shorter wavelengths (Fig. 4).
5. The torsional fast magnetoacoustic wave is more subject to dispersion in the zero-plasma- $\beta$  limit when equilibrium rotation is also present, with diffusive and viscous effects (Fig. 5). For a solar tornado, the dispersion due to magnetic diffusivity is enhanced by the plasma  $\beta$  (Fig. 6). The plasma viscosity enhances the efficiency of the plasma  $\beta$  regarding dispersion effects (Figs. 7 and 8).
6. The damping due to magnetic diffusivity is proportional to the plasma  $\beta$ . Hence, the efficiency of damping is more pronounced in photospheric conditions (Fig. 9). The damping of torsional fast magnetoacoustic waves in solar tornados due to magnetic diffusivity increases with the equilibrium magnetic twist for photospheric and coronal conditions (Fig. 10).
7. The damping due to magnetic diffusivity is stronger in the presence of plasma viscosity for both photospheric and coronal conditions (Figs. 10 and 11). In photospheric conditions, the equilibrium magnetic twist provides stronger damping than in coronal conditions when magnetic diffusivity and plasma viscosity are both present (Fig. 11).

Our findings shed further light on the role of damping effects in addition to atmosphere and equilibrium conditions in modifying the phase speeds and damping of torsional Alfvén waves and torsional magnetoacoustic waves in the context of energy dissipation. The modification of the frequencies and speeds also elevate our knowledge on the spectrum of wavelengths that are affected by dissipation. The damping was also shown to be affected by magnetic twist and plasma rotation, where various modes dissipate subject to atmosphere conditions, providing a sustainable heating mechanism in the solar atmosphere. The relations and dispersion curves enable us to directly estimate the role of the magnetic diffusivity, plasma viscosity, equilibrium magnetic twist, equilibrium plasma rotation, and plasma- $\beta$  conditions on the speed, dispersion, and damping of torsional waves in the linear regime. This in turn provides insight into the speed and lifetime of torsional polarized waves, which are higher and longer at various altitudes in the solar atmosphere. Other damping mechanisms such as resonant absorption, phase mixing, and shock formation, which may all take place in ideal conditions, were

not studied. Thus, the results of our study may not fully govern all observations of propagation and damping of torsional oscillations in the solar atmosphere. The figures showed that the speed strongly increases due to atmosphere and equilibrium conditions. Hence, because large-amplitude perturbations require nonlinear approaches, it will be interesting to carry out numerical simulations to study the connection between dissipative effects in twisted and rotational plasma structures and shock formation.

Finally, we state that the interplay of equilibrium magnetic twist and rotation in addition to magnetic diffusivity and plasma resistivity implies a complex behavior of the energy transfer and transport by torsional waves propagating in solar tornados. In every layer of the solar atmosphere, the interplay of equilibrium and atmosphere conditions enables the ongoing heating of the solar chromosphere and corona, depending to the dominant parametric conditions.

## References

- Alfvén, H., & Lindblad, B. 1947, *MNRAS*, 107, 211
- Aschwanden, M. J. 2005, *Physics of the Solar Corona. An Introduction with Problems and Solutions* (2nd edition)
- Aschwanden, M. J., De Pontieu, B., Schrijver, C. J., & Title, A. M. 2002, *Sol. Phys.*, 206, 99
- Bacri, J.-C., Perzynski, R., Shliomis, M. I., & Burde, G. I. 1995, *Phys. Rev. Lett.*, 75, 2128
- Battaglia, A. F., Canivete Cuissa, J. R., Calvo, F., Bossart, A. A., & Steiner, O. 2021, *A&A*, 649, A121
- Belov, S. A., Vasheghani Farahani, S., & Molevich, N. E. 2022, *MNRAS*, 515, 5151
- Boocock, C., & Tsiklauri, D. 2022a, *MNRAS*, 510, 2618
- Boocock, C., & Tsiklauri, D. 2022b, *MNRAS*, 510, 1910
- Cargill, P. J., De Moortel, I., & Kiddie, G. 2016, *ApJ*, 823, 31
- Chae, J., Litvinenko, Y. E., & Sakurai, T. 2008, *ApJ*, 683, 1153
- Dakanalis, I., Tsiropoula, G., Tziotziou, K., & Koutroumbas, K. 2021, *Sol. Phys.*, 296, 17
- Dakanalis, I., Tsiropoula, G., Tziotziou, K., & Kontogiannis, I. 2022, *A&A*, 663, A94
- De Moortel, I., & Nakariakov, V. M. 2012, *Philos. Trans. R. Soc. Lond. Ser. A*, 370, 3193
- De Pontieu, B., Martens, P. C. H., & Hudson, H. S. 2001, *ApJ*, 558, 859
- Edwin, P. M., & Roberts, B. 1983, *Sol. Phys.*, 88, 179
- Ghoraba, A. M., & Farahani, S. V. 2018, *ApJ*, 869, 93
- Giagkiozis, I., Fedun, V., Scullion, E., Jess, D. B., & Verth, G. 2018, *ApJ*, 869, 169
- Goodman, M. L. 2011, *ApJ*, 735, 45
- Goossens, M. 2003, *An Introduction to Plasma Astrophysics and Magnetohydrodynamics*, Astrophys. Space Sci. Lib., 294
- Goossens, M., Hollweg, J. V., & Sakurai, T. 1992, *Sol. Phys.*, 138, 233
- Hejazi, S. M., Vasheghani Farahani, S., Hajisharifi, K., & Mehdian, H. 2024, *A&A*, 690, A85
- Hejazi, S. M., Vasheghani Farahani, S., & Hajisharifi, K. 2025, *ApJ*, 981, 6
- Heyvaerts, J., & Priest, E. R. 1983, *A&A*, 117, 220
- Ionson, J. A. 1978, *ApJ*, 226, 650
- Kato, Y., & Wedemeyer, S. 2017, *A&A*, 601, A135
- Khodachenko, M. L., Arber, T. D., Rucker, H. O., & Hanslmeier, A. 2004, *A&A*, 422, 1073
- Kolotkov, D. Y., Zavershinskii, D. I., & Nakariakov, V. M. 2021, *Plasma Phys. Controlled Fusion*, 63, 124008
- Komm, R., Gosain, S., & Pevtsov, A. 2014, *Sol. Phys.*, 289, 475
- Kumar, N., & Roberts, B. 2003, *Sol. Phys.*, 214, 241
- Kuniyoshi, H., Shoda, M., Iijima, H., & Yokoyama, T. 2023, *ApJ*, 949, 8
- Leake, J. E., Arber, T. D., & Khodachenko, M. L. 2005, *A&A*, 442, 1091
- Matsuoka, M., Suzuki, T. K., Tokuno, T., & Kakiuchi, K. 2024, *ApJ*, 970, 16
- Mghebrishvili, I., Zaqarashvili, T. V., Kukhianidze, V., et al. 2018, *ApJ*, 861, 112
- Morton, R. J., & Soler, R. 2025, *ApJ*, 986, L6
- Morton, R. J., Sharma, R., Tajfirouze, E., & Miriyala, H. 2023, *Rev. Mod. Plasma Phys.*, 7, 17
- Mozafari Ghoraba, A., Abedi, A., Vasheghani Farahani, S., & Khorashadizadeh, S. M. 2018, *A&A*, 618, A82
- Nakariakov, V. M., & Kolotkov, D. Y. 2020, *ARA&A*, 58, 441
- Nakariakov, V. M., & Roberts, B. 1995, *Sol. Phys.*, 159, 213
- Nakariakov, V. M., Ofman, L., Deluca, E. E., Roberts, B., & Davila, J. M. 1999, *Science*, 285, 862

- Nakariakov, V. M., Verwichte, E., Berghmans, D., & Robbrecht, E. 2000, *A&A*, **362**, 1151
- Nakariakov, V. M., Zhong, Y., & Kolotkov, D. Y. 2024, *MNRAS*, **531**, 4611
- Ofman, L., Nakariakov, V. M., & Deforest, C. E. 1999, *ApJ*, **514**, 441
- Ofman, L., Nakariakov, V. M., & Sehgal, N. 2000, *ApJ*, **533**, 1071
- Pascoe, D. J., Goddard, C. R., Nisticò, G., Anfinogentov, S., & Nakariakov, V. M. 2016, *A&A*, **589**, A136
- Russell, A. J. B., & Fletcher, L. 2013, *ApJ*, **765**, 81
- Selwa, M., & Ofman, L. 2010, *ApJ*, **714**, 170
- Silva, S. S. A., Verth, G., Rempel, E. L., et al. 2021, *ApJ*, **915**, 24
- Skirvin, S. J., Fedun, V., Verth, G., & Ballai, I. 2025, *ApJ*, **988**, 18
- Smith, P. D., Tsiklauri, D., & Ruderman, M. S. 2007, *A&A*, **475**, 1111
- Soler, R., Terradas, J., Oliver, R., & Ballester, J. L. 2017, *ApJ*, **840**, 20
- Soler, R., Terradas, J., Oliver, R., & Ballester, J. L. 2019, *ApJ*, **871**, 3
- Stangalini, M., Erdélyi, R., Boocock, C., et al. 2021, *Nat. Astron.*, **5**, 691
- Tsiklauri, D., Arber, T. D., & Nakariakov, V. M. 2001, *A&A*, **379**, 1098
- Tziotziou, K., Tsiropoula, G., Kontogiannis, I., Scullion, E., & Doyle, J. G. 2018, *A&A*, **618**, A51
- Van Doorselaere, T., Srivastava, A. K., Antolin, P., et al. 2020, *Space Sci. Rev.*, **216**, 140
- Vasheghani Farahani, S., Nakariakov, V. M., & van Doorselaere, T. 2010, *A&A*, **517**, A29
- Vasheghani Farahani, S., Nakariakov, V. M., van Doorselaere, T., & Verwichte, E. 2011, *A&A*, **526**, A80
- Vasheghani Farahani, S., Ghanbari, E., Ghaffari, G., & Safari, H. 2017, *A&A*, **599**, A19
- Vesa, O., Shetye, J., & Verwichte, E. 2025, *MNRAS*, **543**, 3152
- Wedemeyer, S., & Steiner, O. 2014, *PASJ*, **66**, S10
- Wilmot-Smith, A. L., Priest, E. R., & Hornig, G. 2005, *Geophys. Astrophys. Fluid Dyn.*, **99**, 177
- Zaqarashvili, T. V., Khodachenko, M. L., & Rucker, H. O. 2011, *A&A*, **529**, A82
- Zhong, Y., Kolotkov, D. Y., Zhong, S., & Nakariakov, V. M. 2023, *MNRAS*, **525**, 5033
- Zhugzhda, Y. D. 1996, *Phys. Plasmas*, **3**, 10
- Zhugzhda, Y. D., & Nakariakov, V. M. 1999, *Phys. Lett. A*, **252**, 222